Full-Duplex Operation in Two-Way Broadcast Service for Maritime Applications

Tomás Ramírez, Carlos Mosquera
Signal Theory and Communications Department
University of Vigo
36310 - Vigo, Spain
Email: {tramirez,mosquera}@gts.uvigo.es

***Abstract*—A system analysis of the operation of the new VDES standard is made, with special attention to the comparison between full-duplex and half-duplex operation at the satellite. We analyze both uplink and downlink transmissions when broadcast traffic is transmitted in the downlink. The self-interference from the satellite transmitted signal will be the main impairment for the full-duplex operation. Results show that full-duplex can outperform half-duplex in the uplink for low to moderate levels of self-interference. In the downlink, full-duplex nearly doubles the capacity of half-duplex. We also recommend some updates to the standard VDES to reduce the impact of self-interference in the performance of the full-duplex mode.**

I. Introduction

In the maritime Very High Frequency (VHF), Automatic Identification System (AIS) [1] service has found a widespread use since its implementation some years ago. AIS service is employed for the safety of vessels and collision avoidance, by exchanging ship data such as position or course with nearby ships and coast stations. Furthermore, AIS has the capability to exchange complementary navigation information by means of application-specific messages (ASM). In recent years multiple AIS related standards have emerged making use of the ASM capability, such as AIS AtoN (AIS Aid to Navigation), AIS SART (AIS Search and Rescue Transmitter), AIS MOB (AIS Man Overboard) or EPIRB AIS (Emergency Position-Indicating Radio Beacons AIS). This is causing the network overloading of the AIS channels, compromising the proper functionality of safety monitoring systems associated with AIS. In order to avoid this, the idea of moving novel AIS applications and ASM to other channels has been proposed. The alternative is to use additional maritime VHF channels for VHF data exchange (VDE) [2]. This would allow the use of the existing VHF infrastructure on the ships with minor modifications for VDE services.

In Figure 1 the resource channel allocation of the VHF data exchange system (VDES) is presented. The channelization in VDES is such that terrestrial and satellite signals can mutually interfere. The resource sharing method can avoid the interference by exclusive time and frequency allocation; this is the case of initial resource sharing configuration, a static allocation for situations where shore station and satellite are not coordinated. In the satellite-to-earth and shore-to-ship (and ship-to-ship) band, we assume that 50 KHz are exclusively assigned to VDE-SAT downlink (channels 2026 and 2086) and 100 KHz for VDE-Terrestrial (channels 2024-2025 and 2084-2085). At the lower frequency leg, 50 KHz (channels 1026 and 1086) are of exclusive use for the VDE-SAT uplink, whereas 100 KHz are assigned to ship-to-shore communications. On the other hand, legacy ASM (channels 2027 and 2028) and AIS have specific frequency bands. Even though terminals at ships are half-duplex (HD), without simultaneous transmission and reception capability, the standard does not preclude this option at the satellite. The term Full Duplex (FD) is commonly used to refer to the simultaneous transmission and reception, either in separate time slots or different frequency bands. More recently, a new paradigm known as In-band Full Duplex (IBFD) has been proposed [3], advocating for the simultaneous use of the same frequency band for both transmission and reception. In this paper, FD refers to the simultaneous transmission and reception taking place in a Frequency-Division Duplexing (FDD) system, with different frequency channels allocated to uplink and downlink, as detailed above for VDE-SAT. The main source of degradation in IBFD transceivers is the coupled signal which the receiver picks from the transmitter. This signal, known as Self-Interference (SI), can overwhelm the received signal from the other end, disrupting the communication if proper attenuation is not enforced. To a lesser extent, this problem arises also in FDD transceivers when the separation between transmit (TX) and receive (RX) frequency bands is not sufficient to guarantee the blocking of the coupling by passive filters. Significant spectral content can be generated at the output of the power amplifier contaminating near channels; this out-of-band noise can even mask the received signal in FDD, as illustrated in Figure 2. If the satellite operates in FD mode, recepction in the near AIS and ASM channels can be affected. Even further, the VDE-SAT uplink band is expected to suffer interference to some extent, due to the large gap between the transmit and received powers (roughly 150 dB with data taken from [2]). When passive attenuation alone cannot reduce the coupling down to a tolerable level, then active cancellation schemes can be devised to contribute to the required attenuation. In this sense there exist many commonalities with IBFD cancellation schemes, which have received strong attention during the last few years due to the potential benefits for reusing the spectrum. In [4] a recent state of art of cancellation systems is presented, which can be taken as reference. Active cancellation is a complex process with implementation constraints. The amount of residual SI will determine the performance of the FD VDE-SAT link. In this paper we realize an initial analysis of relative performance of FD and HD for the new VDE-SAT service; the impact of VDE-SAT on AIS and ASM will be out of the scope of this work. Both Demand Assigned and Random Access multiple access

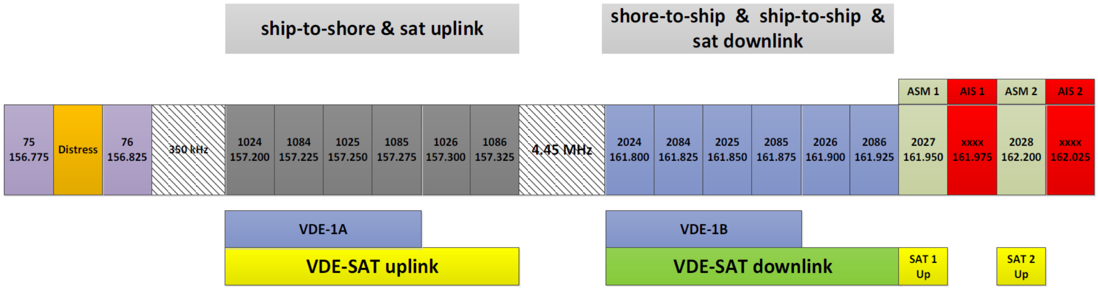

Fig. 1: VDES resource allocation [2].

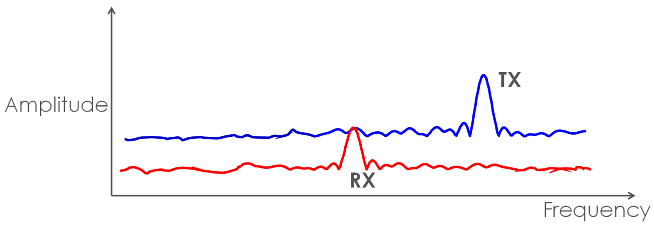

Fig. 2: Tx and Rx bands do not overlap, although the out-of-band noise extends over a significant amount of spectrum.

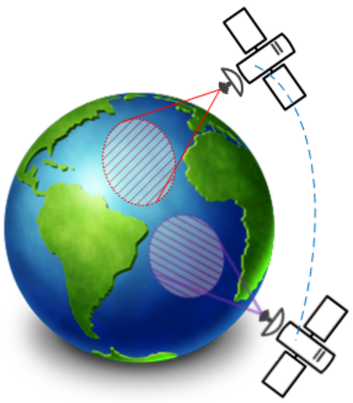
Fig. 3: LEO satellite footprint.

mechanisms are included in the study, and the performance of FD and HD is compared. Moreover, a simplified simulator of VDE-SAT is implemented.

The paper is organized as follows. Section II presents the VDE-SAT system model. Section III contains a preliminary analysis of VDE-SAT, with simulation results detailed in Section IV before summarizing the conclusions.

II. VDE-SAT Model

The study will consider one pass of a LEO satellite (Figure 3), in the understanding that the uplink capacity can be increased if more satellites offer the service. Vessels are randomly distributed in the area with satellite visibility, following a uniform pattern for simplicity. The VDES frame structure is identical to that in AIS, and also synchronized in time on the Earth surface to UTC. Each frame consists of 2250 slots spanning one minute. Figure 4 shows the frame structure for both uplink (UL) and downlink (DL) slots in VDES. Each division in the figure occupies 90 slots, corresponding to the extension of downlink PL-Frames. Equivalently, this amounts to three uplink frames. PL-Frames are the transmissions modes of uplink and downlink defined in the VDES standard [2]. Logical channels are blue coloured, in particular, the Bulletin Board Signalling Channel (BBSC) and the Announcement Signalling Channel (ASC). BBSC defines the network configuration parameters such as signalling channels and data channels, protocol versions and future network configuration. ASC carries announcements, MAC information, and up/downlink resource allocation, ARQs, ACKs and EDNs. Since vessel terminals are HD, they are not available for transmission during the reception of these logical channels, and as such are labelled as red in the figure. Additional reductions due to the need of the ship terminals to listen to other services such as AIS are not included in this study. Moreover, we assume broadcast traffic in the downlink, labelled as *Bro* in Figure 4. On the other hand, unicast traffic is considered in the uplink for request transmissions and data transmissions. [2]. In order to gain access to the Access Demand Channels (ADC), vessels will have to realize a previous request through the Random Access Resource Request Channel (RQSC). A good account of random access (RA) protocols specially suited for satellite communications, starting with basic Slotted Aloha (SA), and covering enhanced versions based on iterative detection, for both TDMA and CDMA, is presented in [5]. Two types of traffic, Poisson and bursty, the latter based on a modified version of the Web traffic model, are considered in [5]. As random access scheme, we will assume Slotted-Aloha. If a transmission request is correctly received by the satellite, a demand access channel will be assigned and informed in ASC. Therefore it is expected that uplink resource occupation will depend on the random access scheme used and on the input traffic load. In order to provide the same capability for accepting requests, an equal number of RQSC channels will be allocated in both HD and FD frames for the simulations. A careful look at Figure 4 shows 21 downlink Broadcast channels and 57 uplink Demand access channels in FD. In the HD case, for performance comparison, we will assume a balanced distribution of resources, with 9 downlink Broadcast channels and 30 uplink Demand access channels. Tables I and II summarize the PL-Frames used in this paper. The simulation of uplink transmissions in DA channels and uplink requests in RQSC channels will use PL-Frame 5 and PL-Frame 3, respectively, whereas the BBSC transmissions and broadcast transmissions in the downlink will use PL-Frame 1 and PL-Frame 2, respectively.

The simulation will take place at the link layer, with an abstraction model for the physical layer; the Signal-to-Interference and Noise Ratio (SINR) will be used to decide

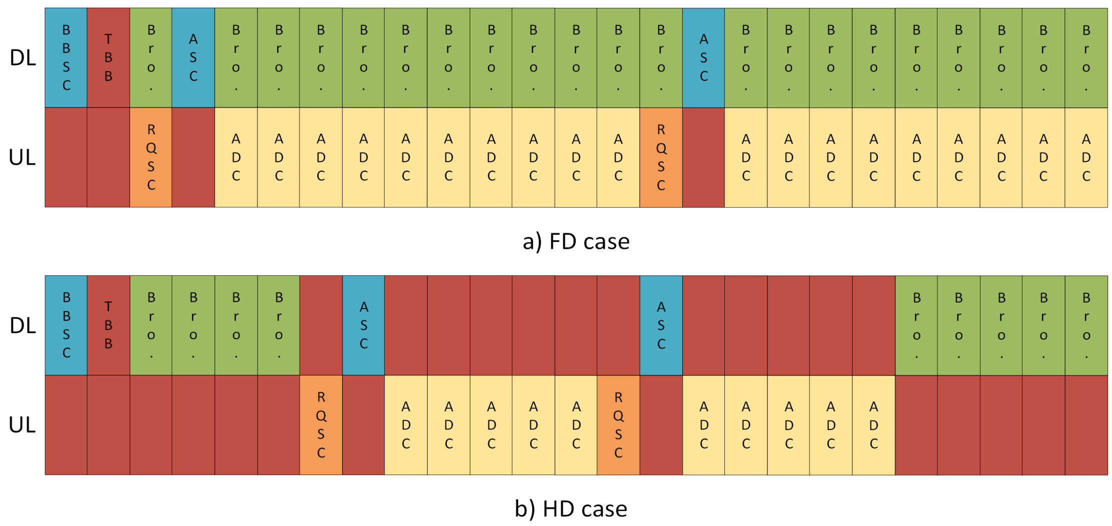

Fig. 4: VDES frame structure.

whether the corresponding PL-Frame is correctly decoded based on its minimum required SINR. The expression for the SINR is given by

$$SINR(t) = \frac{p_t \cdot g_{sat}(t) \cdot g_{ship}(t) \cdot l_{prop} \cdot l_{channel}}{k \cdot T \cdot B + I} \quad (1)$$

where p_t is the transmission power, g_{sat} the satellite antenna gain, g_{ship} the ship antenna gain, l_{prop} the propagation losses, k the Boltzmann constant, T the noise temperature of the receiver, B the bandwidth, I the interference level and $l_{channel}$ the additional channel losses. The received power will be a function of the geometry of the link (position of the vessel within the satellite footprint) and the fading caused by local reflections. The channel follows a Rician model with carrier to multipath ratio equal to $\frac{C}{M} = 10$ dB [2], which is assumed independent for the different vessels. In uplink, SI due to the simultaneous transmission and reception by the satellite will be added to the receive noise in the FD case. The amount of SI will be a parameter of the study, since it is very difficult to anticipate how much transmit power will be leaked into the receiver on an accurate basis, even if some sort of cancellation schemes are implemented. SI level will be determined by β, the SI relative power with respect to the satellite noise floor $N_{SAT} = k \cdot T_{sat} \cdot B$:

$$I = \beta \cdot N_{SAT}. \quad (2)$$

Besides SI in the FD scenario, operation in FD mode raises another issue, the cross-interference among terminals [6]: a given terminal can transmit while another one is receiving, since the satellite operates in FD mode. The corresponding interference levels can be estimated by using the recommendation ITU-R P.1546-5 [7] if the out-of-band emissions of the vessels terminals are known. The cross-interference will be a function of several factors such as uplink load traffic or vessels distance distribution. Both self-interference and cross-interference will determine how far from the promised doubling of the half-duplex capacity the system performance is.

The SI on the satellite will restrict the FD performance due to the SINR requirement of PL-Frames. The current version of the VDES standard [2] does not preclude the use of FD, although includes a very limited set of PL-Frames which would not be robust enough to cope with the additional interference. According to [2], BBSC allocates the available PL-Frames to the different ADC at the beginning of each frame. The balance of PL-Frames within a frame should anticipate somehow the diversity of service demands from the ship terminals in terms of spectral efficiency. For the purpose of the simulation, we will choose the PL-Frame for each user SINR on-the-fly, thus exploiting better each user channel. We will assume a perfect knowledge of the SINR to choose the corresponding uplink PL-Frame, although in practice some errors in the estimation together with a time variation of the channel quality could require the use of a protection margin[1]. For exploring the potential gain accrued from the use of FD mode, we will define an additional PL-Frame for ADC and request channels, detailed in Table III.
The data traffic generated by each vessel will follow a Poisson distribution for our simulations. The traffic load will be such that two cases will be simulated: a low load (LL) case, demanding full use of ADC channels in HD mode and approximately 50% in FD mode, and a high load (HL) one demanding full use of ADC channels in FD. Unsuccessful PL-Frames in ADC channels will be considered as lost. The metric of the simulation will be the ratio between the HD and FD respective throughputs.

TABLE I: Downlink PL-Frames [2].

	PL-Frame 1	PL-Frame 2	
MODCOD	BPSK	QPSK	
FEC Rate	1/2	1/4	
Spreading Factor	8	1	
Unfaded C/N_0	43	43	dBHz
Burst Duration	90	90	slots
Number of info bits	4480	20480	bits

Next section details some analysis results to support the simulations, which will be presented in Section IV.

[1]For the case of uplink random transmissions, an open loop estimate might be more practical, with the terminals choosing the transmission PL-frame based on the quality of their received signal. A related idea for DVB-SH/E-SSA forward/return links is presented in [8], in this case for conventional half-duplex duplexing. Here some a priori knowledge about the on-board degradation due to SI would be needed.

TABLE II: Uplink PL-Frames [2].

	PL-Frame 3	PL-Frame 4	PL-Frame 5	
MODCOD	OQPSK	16APSK	16APSK	
FEC Rate	3/4	3/4	3/4	
Unfaded C/N_0	73	73	73	dBHz
Burst Duration	1	1	90	slots
Number of info bits	256	512	69936	bits
Information rate	50.4	100.8	100.8	kbits/s

TABLE III: New Uplink PL-Frame definitions.

MODCOD	OQPSK	OQPSK	
FEC Rate	3/4	3/4	
Unfaded C/N_0	67	67	dBHz
Burst Duration	1	90	slots
Number of info bits	256	34968	bits
Information rate	50.4	50.4	kbits/s

III. ANALYSIS OF VDES

For a proper understanding of the VDES operation, we make a preliminary simplified analysis in this section to obtain some insights on the FD vs. HD performance, before presenting the simulations in next section. As mentioned earlier, the current definition of the standard [2] specifies very few PL-Frames, with a very limited number of transmission rates to choose from. In consequence, for analysis purposes we use the channel capacity expression instead to estimate the potentially achieved rates. The SINR, obtained with (1), will be used to compute the capacity:

$$C(t) = K \cdot log_2(1 + SINR(t)) \quad \left[\frac{bps}{Hz}\right]. \tag{3}$$

A convenient gap factor could be included to obtain a better prediction of the achievable rates in practice, to account for the distance between the practical codes and the Shannon limit. Given the short list of defined rates in the standard, we have not resorted to this approach, keeping in mind that the presented throughput values will be an upper bound for practical results. The factor K will depend on the specific case, for example, the allocated time to each transmission direction in the HD case. The SINR distribution will be obtained from the satellite footprint, by considering the Earth as a perfect sphere, and assuming that the LEO satellite orbit has constant height. Thus, the metrics that we obtain will be independent of the footprint location. The SINR statistics will determine the outage capacity, i.e., the capacity that can be achieved with a certain probability. For analytic results an outage probability of 0.01 is considered, and uplink traffic will be reduced to unicast transmissions in ADC channels. As pointed out earlier, vessels need to use the RQSC to request slots for sending information in ADC channels. In this model, we will assume that all requests leading to a full occupancy of uplink resources by unicast transmissions can be managed by the RQSC. Outage capacity will be used to compare the performance between HD and FD in both uplink and downlink. The duration of the uplink transmissions from the vessels will be a key parameter to obtain the average number of lost downlink transmissions, since vessels operate in HD mode, and cannot transmit and receive simultaneously.

A. HD Case

Available slots in a VDES frame are shared between uplink and downlink, not necessarily in equal terms. The K factor in (1) is detailed in Table IV for different sharing ratios. The fractional amount of time allocated to the uplink is denoted by t_{ul}.

TABLE IV: K factor in HD case.

t_{ul}, relative uplink allocation	Number of 90-slot groups for uplink	Uplink K factor	Number of 90-slot groups for downlink	Downlink K factor
0.0455	1	0.04	21	0.84
0.0909	2	0.08	20	0.8
0.1364	3	0.12	19	0.76
0.1818	4	0.16	18	0.72
0.2273	5	0.20	17	0.68
0.2727	6	0.24	16	0.64
0.3182	7	0.28	15	0.60
0.3636	8	0.32	14	0.56
0.4091	9	0.36	13	0.52
0.4545	10	0.40	12	0.48
0.5	11	0.44	11	0.44
0.455	12	0.48	10	0.40
0.5909	13	0.52	9	0.36
0.6334	14	0.56	8	0.32
0.6818	15	0.60	7	0.28
0.7273	16	0.64	6	0.24
0.7727	17	0.68	5	0.20
0.8182	18	0.72	4	0.16
0.8636	19	0.76	3	0.12
0.9091	20	0.8	2	0.08
0.9545	21	0.84	1	0.04

B. FD Case

All slots can be used in both directions, except those already mentioned with signalling information, which pose a 12% overhead. With this, the K factor for both uplink and downlink is 0.88. The HD operation of the vessel terminals prevents them from receiving the DL information while transmitting. This will entail a reduction on the capacity transmission of the downlink due to the effective listening reception time, decreased due to the impossibility of transmitting and receiving simultaneously. The erasure of the downlink channel will be accounted by an additional reduction of the capacity to be computed. This reduction is highly dependent on the capacity of the uplink, since the time employed for UL transmissions will be a direct function of the spectral efficiency and the volume of data to transmit. Not surprisingly, the uplink capacity in FD will depend on the SI level, which can significantly degrade the SINR. In order to obtain an approximation of this capacity reduction in downlink, we define the duration of the ships uplink transmission as

$$Number\ of\ blocks = \left\lceil \frac{N}{t_{data} \cdot B \cdot C_{UL}} \right\rceil \tag{4}$$

where N is the volume of data in bits, t_{data} the transmission time of data in seconds, B is the transmission bandwidth in Hz and C_{UL} is the spectral efficiency of the uplink in bits/s/Hz. For numerical results, we will assume that each ship needs to transmit a data volume equal to that in PL-Frame 5.

The corresponding capacity distribution, from (3), will yield the required uplink transmission blocks to transmit the specified data volume. Note that an uplink transmission block corresponds to 30 slots, the transmission length for uplink PL-Frames in ADC channels. The number of uplink transmission blocks is distributed according to Figure 5 for

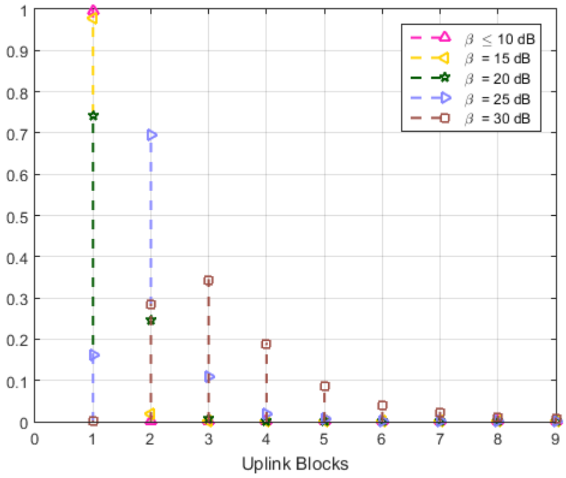

Fig. 5: Probability Mass Function of uplink transmissions.

different amounts of interference. The SINR margin is such that for $\beta \leq 10$ dB no additional transmissions are required. We need to keep in mind that β represents the additional level of the interference with respect to the noise. Higher interference values require extra redundancy to guarantee the communication, occupying more uplink blocks. In turn, the downlink capacity will get affected as pointed out before, since the terminals cannot receive for longer periods of time. Table V shows the average number of downlink lost blocks assuming total occupation of ADC channels and same duration in all transmissions, with K_{DL_i} denoting the percentage of downlink blocks received. Although apparently counterintuitive, we assume an alignment such that only one DL block is affected when three UL blocks are needed to transmit the required volume of data.

With Table V and probability distribution in Figure 5, the downlink capacity reduction factor can be approximated by:

$$K_{FD} = p_1 \cdot K_{DL_1} + \quad p_2 \, K_{DL_2} + \ldots + p_i \cdot K_{DL_i} \qquad (5)$$

where p_i is the probability of requiring i uplink blocks. In Table VI the downlink capacity reduction factor is obtained for different values of β. As a result, the factor K to be used in (1) for the FD DL is $K = 0.88 \cdot K_{FD}$. We are neglecting the potential interlink interference in the FD mode coming from the only vessel which is transmitting at a time.

TABLE V: Additional factor for DL lost transmissions.

UL blocks	Lost DL blocks (average)	K_{DL_i}
1	1	0.9545
2	1.5	0.9318
3	1	0.9545
4	2	0.9091
5	2.5	0.8864
6	2	0.9091
7	3	0.8636
8	3.5	0.8409
9	3	0.8636

TABLE VI: Downlink capacity reduction caused by uplink transmissions.

β	$-\infty$	0	5	10	15	20	25	30
K_{FD}	0.9545	0.9545	0.9545	0.9544	0.954	0.948	0.935	0.91

C. FD vs. HD

The gain ratio of outage capacity 0.01 for uplink and downlink are presented in Figures 6 and 7, respectively. For the HD case, $t_{UL} = 0.5$ was assumed. In the uplink, HD will outperform FD for interference levels higher than 12 dB. If interference levels are lower than 12 dB, then more time needs to be allocated to the uplink to match the FD capacity, thus penalizing the downlink capacity. Moreover, capacity is doubled for $\beta = -\infty$ (not shown in the figure) as expected. In the downlink, FD always performs better than HD. There is a small dependency with the SI level due to the additional redundancy required to compensate for the erasures in the terminals, caused by the extra transmission time needed to cope with the degraded SINR. However, this dependency is barely significant, not enough to compromise the FD performance in comparison with HD.

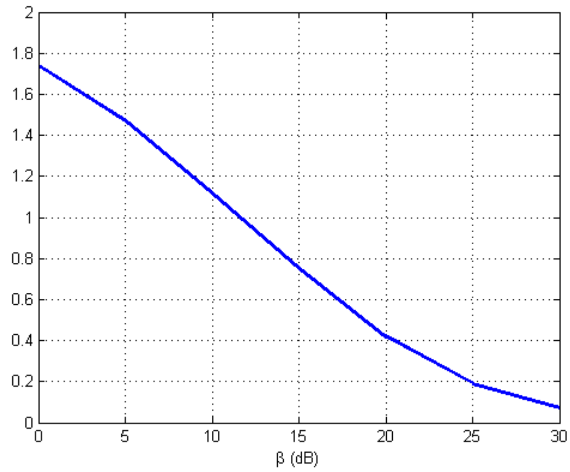

Fig. 6: Ratio between FD and HD uplink outage capacities. Broadcast traffic in downlink and unicast traffic in uplink.

IV. Simulation Results

Next we simulate the performance of VDE-SAT for both FD and HD modes, following the set-up introduced in Section

TABLE VII: Monte-Carlo simulations set-up for Section IV.

Number of simulations	300
Simulation setting	- Simulation area: latitude extent 40^o, longitude extent 20^o - A given number of ships is distributed uniformly - Relative ship and satellite location determines the SINR level - Two cases are simulated: (i) PL-Frame is fixed in BBSC; (ii) PL-Frames are adapted according to SINR
Random components in simulation	- Vessel location in area - Data traffic generation - SA access in RQSC channels

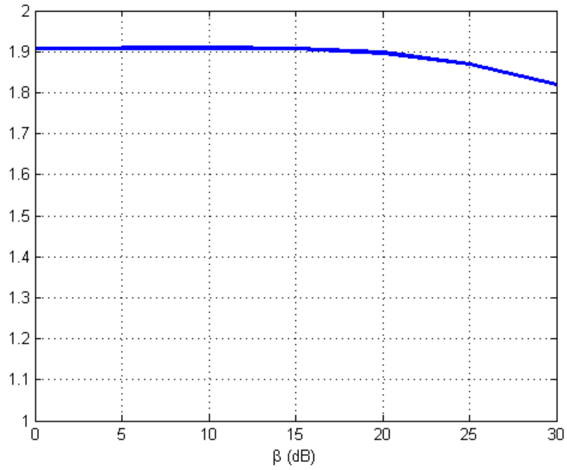

Fig. 7: Ratio between FD and HD downlink outage capacities. Broadcast traffic in downlink and unicast traffic in uplink.

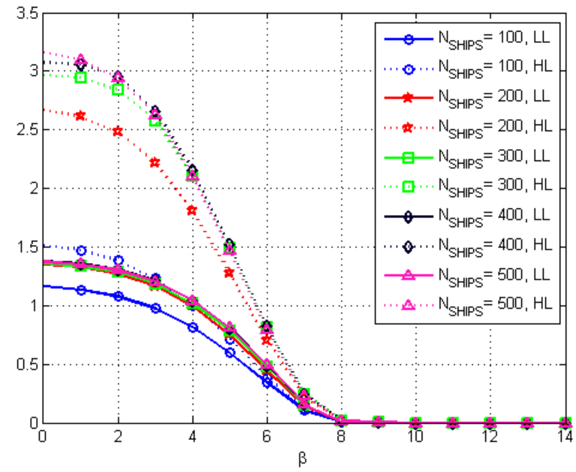

Fig. 8: Ratio between FD and HD uplink throughput, with fixed PL-Frame.

II. For HD operation, the resource allocation will be equal for both UL and DL, so that $t_{ul} = 0.5$. The number of Monte-Carlo realizations was 300 in all cases, with vessels randomly placed for each run, as summarized in Table VII.

A. Uplink

Results for a fixed PL-Frame are presented in Figures 8 and 9, where N_{SHIPS} is the number of ships in the area, and LL denotes the low load case and HL the high load case. As expected, FD has a better performance than HD for low levels of SI, with a decreasing gain for higher levels of SI, turning into loss when the curves drop below one. With respect to the ratio value, a 100% throughput gain is expected for low levels of β due to resources distribution in HD, as anticipated by results with only ADC channels in Figure 6. Nonetheless, simulation results in Figure 8 display ratio values higher than two for some cases. This is due to the degradation of HD performance for a high input load. In practice, the system would be nearly saturated when achieving this operating point, an undesired situation for both HD and FD. This degradation comes from the delay between assignment and transmission in the ADC channel. For high input loads, HD satellite cannot assign all requests in the same frame, deferring transmissions for subsequent frames. As a result, uplink transmissions can be lost due to insufficient SINR to decode the corresponding PL-Frame when the ADC channel is assigned.

Furthermore, we can observe how FD performance is totally degraded with β levels above 7 dB. This degradation of FD performance can be noticed from the average ADC occupation in Figure 9, with ADC channels not being assigned for β levels above 7 dB. If in addition to PL-Frame 5 we can choose the more robust PL-Frame defined in Table III, then there is an improvement for higher SI values, as we can observe in Figure 10. FD operation range is extended till $\beta \approx 14$ dB. FD performance is now almost equal to that in HD for the interval $7 \leq \beta \leq 14 dB$.

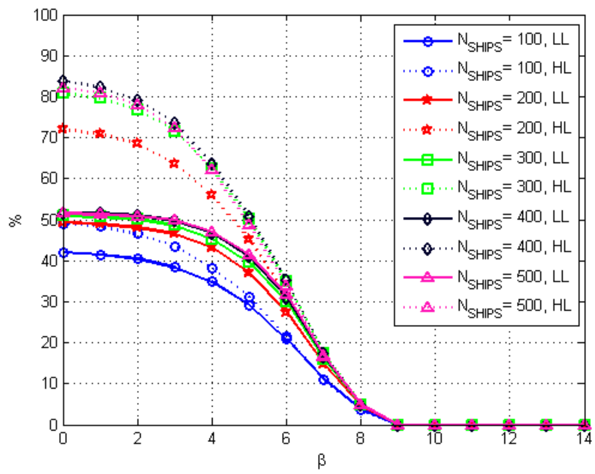

Fig. 9: Average ADC occupation in FD for a fixed PL-Frame.

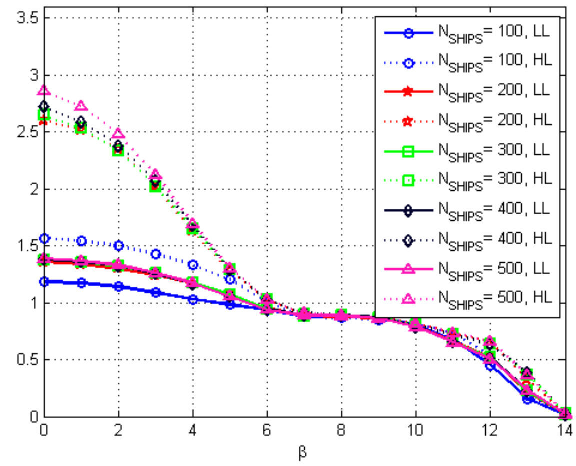

Fig. 10: Ratio between FD and HD uplink throughput, with adaptive PL-Frame.

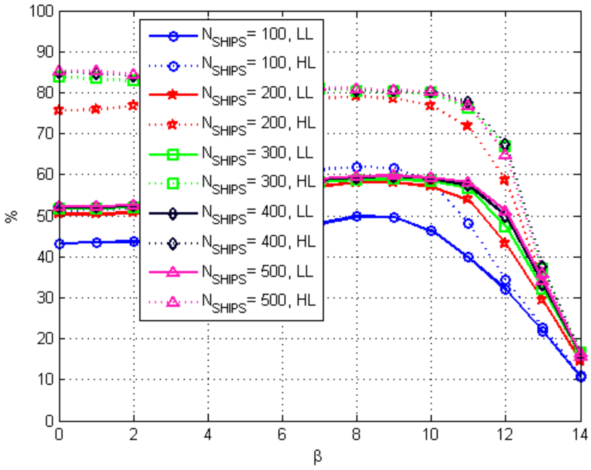

Fig. 11: Average ADC occupation in FD for adaptive PL-Frame.

B. Downlink

Keeping in mind that, for the simulation, 21 downlink Broadcast channels are assigned to FD and 9 Downlink Broadcast channels are assigned to HD, we have a downlink theoretical ratio of $21/9 = 2.333$. Simulation results were such that the ratio was about 90% of that value. The same trend applies to the resource occupation, with the analysis showing a potential doubling of the HD performance, and simulations not shown here yielding ratios in the order of 1.85-1.9.

V. Conclusions

A system analysis and simulation of VDE-SAT was presented to obtain the exchange of information limits between a LEO satellite and the vessels on a given area. The abstraction of the physical layer left as random elements of the study the location of the vessels, the fading of the channel, and the traffic generated by the terminals. The new standard does not preclude the operation of the satellite in FD mode, so a performance comparison was made between both FD and HD operation modes, in an effort to understand the potential benefits of the simultaneous transmission and reception under the additional self-interference on the satellite. All throughout the paper the self-interference was parameterized by its relative power level with respect to the noise floor. In practice, this power will be possibly the residue after some passive and active countermeasures to attenuate the coupling of the transmitted signal. For low to moderate amounts of self-interference, FD outperforms HD as expected, especially if the initial proposal of PL-Frames currently defined in the VDES recommendation is enlarged. Thus, more robust PL-Frames could allow the operation in lower SINR conditions due to the self-interference, and still provide a higher throughput due to the FDD operation with respect to HD switching between uplink and downlink.

Acknowledgement

Work supported by the European Space Agency under ESTEC Contract No. 400113177/15/NL/CLP: SATNEX-IV, and by the European Regional Development Fund (ERDF) and the Spanish Government under project TACTICA and COMPASS (TEC2013-47020-C2-1-R), by the Galician Regional Government and ERDF under projects Consolidation of Research Units (GRC2013/009), REdTEIC (R2014/037) and AtlantTIC. The authors are also grateful to Nader Alagha, from the European Space Agency, for his motivation and recommendations. The view expressed herein can in no way be taken to reflect the official opinion of the European Space Agency.

References

[1] *Technical characteristics for an automatic identification system using time division multiple access in the VHF maritime mobile frequency band*, ITU-R M.1371-5, 2014.

[2] *Technical characteristics for a VHF data exchange system in the VHF maritime mobile band*, ITU-R M.2092-0, October 2015.

[3] D. Bharadia, E. McMilin, and S. Katti, "Full duplex radios," in *Proceedings of the ACM SIGCOMM 2013 Conference on SIGCOMM*, ser. SIGCOMM '13. New York, NY, USA: ACM, 2013, pp. 375–386. [Online]. Available: http://doi.acm.org/10.1145/2486001.2486033

[4] Z. Zhang, K. Long, A. V. Vasilakos, and L. Hanzo, "Full-duplex wireless communications: Challenges, solutions, and future research directions," *Proceedings of the IEEE*, vol. PP, no. 99, pp. 1–41, 2016.

[5] R. De Gaudenzi and O. del Rio Herrero, "Advances in random access protocols for satellite networks," in *Satellite and Space Communications, 2009. IWSSC 2009. International Workshop on*, Sept 2009, pp. 331–336.

[6] X. Xie and X. Zhang, "Does full-duplex double the capacity of wireless networks?" in *INFOCOM, 2014 Proceedings IEEE*, April 2014, pp. 253–261.

[7] *Method for point-to-area predictions for terrestrial services in the frequency range 30 MHz to 3 000 MHz*, ITU-R P.1546-5, September 2013.

[8] O. Del Rio Herrero and R. De Gaudenzi, "High efficiency satellite multiple access scheme for machine-to-machine communications," *Aerospace and Electronic Systems, IEEE Transactions on*, vol. 48, no. 4, pp. 2961–2989, October 2012.